Comparative Influence of Snow and SST Variability on Extratropical Climate in Northern Winter

ARUN KUMAR AND FANGLIN YANG*

National Centers for Environmental Prediction, Climate Prediction Center, Washington, D.C.

(Manuscript received 13 March 2002, in final form 5 September 2002)

ABSTRACT

In this study the influence of snow on atmospheric seasonal mean variability in the extratropical latitudes during boreal winter was studied. The motivation for this analysis was to understand the characteristics of low-frequency atmospheric variability in the extratropical latitudes, and to assess if the interannual variations in snow could lead to potential predictability on seasonal timescales. The influence of snow on atmospheric variability was assessed from a suite of atmospheric general circulation model (GCM) simulations where snow depth amount was either prescribed to a seasonally varying climatology, or was allowed to evolve during the model integration. Further, the influence of snow variability was contrasted with the influence of interannual variability in sea surface temperatures (SSTs) on the atmospheric flow.

A systematic influence of snow variability on the atmospheric seasonal mean variability was found. For example, for the GCM simulations in which snow amount and its extent were allowed to evolve freely, the interannual variability of surface air temperature was found to be larger. The influence of snow variability, however, was confined to the lower troposphere, and little change in the interannual variability of upper-tropospheric circulation, for example, 200-hPa heights, occurred. This bottom-up vertical structure of the influence of snow on the atmospheric variability was in contrast to the top-down influence of tropical SST variability on the extratropical flow.

The cause for the enhancement of atmospheric variability in the lower troposphere was argued to be related to the dependence of surface albedo on snow depth amount. This dependence was such that the interaction between the atmospheric variability and the underlying snow could be viewed as a positive feedback process whereby surface temperature anomalies amplify even further.

1. Introduction

In the extratropical latitudes, the interannual variability of seasonal mean atmospheric states is made of the variability internal to the atmosphere, and variability forced by the changes in the boundary forcing, for example, sea surface temperatures (SSTs). How atmospheric variability affects the underlying surface, and how the changes in the surface feedback affect the atmospheric variability, are interesting scientific questions of relevance toward predictability of seasonal means, and the understanding of the nature of low-frequency variability in the extratropical latitudes.

Along these considerations, interactions and feedbacks between the extratropical oceans and the atmosphere have long been studied (Gallimore 1995; Barsugli and Battisti 1998; Bladé 1997; Bhatt et al. 1998; Kushnir et al. 2002). Results from these studies have demonstrated that for seasonal timescales, interactions between the atmosphere and ocean, and associated changes in the extratropical SSTs, lead to an increase in the amplitude of atmospheric variability. The physical mechanism for this increase is shown to be related to a reduction in thermal damping of the atmospheric variability by the surface energy fluxes.

It is also well known that influences of the interannual changes in the tropical Pacific SSTs, via the atmospheric bridge mechanism, induce extratropical SST anomalies (Lau and Nath 1996). These SST anomalies can also modulate the extratropical atmospheric variability, and therefore, provide an additional mechanism whereby, influencing the atmospheric response to tropical SST forcing, extratropical SSTs can also affect extratropical atmospheric variability.

Similar interactions and feedbacks between atmospheric variability and land can also occur. For boreal winter, a likely candidate among different land surface processes that can play a role in modulating the atmospheric variability is the interaction between snow amount and lower-tropospheric temperatures. Many as-

* Current affiliation: NASA Goddard Space Flight Center, Climate and Radiation Branch, Greenbelt, Maryland.

Corresponding author address: Dr. Arun Kumar, National Centers for Environmental Prediction, Climate Prediction Center, 5200 Auth Road, Camp Springs, MD 20746.
E-mail: arun.kumar@noaa.gov

TABLE 1. Characteristics of GCM simulations used in this study.

GCM simulation	SST specification	Snow specification	No. of simulations	Period of integration
SST_SNO	Observed	Predicted	3	1950–99
SST_CSNO	Observed	Climatological	3	1950–99
CSST_SNO	Climatological	Predicted	1	150 yr
CSST_CSNO	Climatological	Climatological	1	150 yr

pects of interaction between the snow and atmospheric circulation have been studied earlier (for a recent review see Cohen and Entekhabi 2001). In general, such studies fall under two categories. In the first, from the use of the observed snow amount and the atmospheric circulation data, relationships between their interannual variability are analyzed (Walland and Simmonds 1997; Clark et al. 1999). Such analysis, however, suffers from the lack of reliable snow records, and further, causal relationships between the atmospheric and the snow variability are difficult to identify. The second category of studies involves the use of GCM simulations where the influence of specified anomalous snow conditions on the atmospheric circulations is investigated (Walsh and Ross 1988; Barnett et al. 1998; Wanatabe and Nitta 1998; Cohen and Entekhabi 1999, 2001). A drawback of such studies has been that they often rely on specification of extreme, and often unrealistic, snow anomaly conditions. In this paper we attempt to bridge the gap between the two categories of analysis. Following the approach used in understanding the interaction and feedbacks between the extratropical oceans and the atmosphere, an attempt is made to document how the interannual variability in snow depth modulates the extratropical atmospheric variability on seasonal timescales in boreal winter. A comparison of the influence of snow variability on the atmospheric circulation with the corresponding influence of tropical SST variability is also made.

From a suite of atmospheric GCM simulations, where different specifications of snow were made, the influence of snow variability on the variability of seasonal atmospheric means in the extratropical latitudes is analyzed. Because tropical SSTs also affect the extratropical atmospheric variability, an assessment of the relative influences of snow and remote SST variability on the extratropical atmospheric seasonal means is also made. Atmospheric GCM simulations and analysis procedures are described in section 2. The results are presented in section 3. A physical explanation for how the snow variability influences the atmospheric variability is discussed in section 4. A summary, discussion, and some concluding remarks are given in section 5.

2. GCM simulations

The atmospheric GCM used in this study was the seasonal forecast model at the National Centers for Environmental Prediction (NCEP), and is described in detail by Kanamitsu et al. (2002). In brief, the GCM has a spectral triangular truncation at wavenumber 42 (T42), and has 28 levels in the vertical direction. The horizontal grid spacing is approximately 3° in latitude and longitude. The GCM also includes detailed parameterizations of different physical processes in the atmosphere.

Parameterizations of particular relevance to this study are snow budget and surface albedo. The treatment of snow is simple, and in many aspects, common to other GCMs (see Foster et al. 1996). Snow mass on the ground is governed by a prognostic equation that includes snow accumulation, melting, and sublimation. Snow accumulates if precipitation falls and the lower-tropospheric temperature near the surface is below 0°C. The source of energy required for snow melting and sublimation is from radiation and underlying soil. Surface albedo over snow-covered surface is parameterized, and only depends on snow depth (see the appendix). The effect of snow aging is not considered. Finally, fractional snow cover is determined by snow depth and surface roughness [Eq. (A2)].

Our analysis is based on four sets of GCM simulations, which differed in their specifications of either SST or snow variability. These simulations are described in Table 1. The first two sets of simulations were forced with the same global distribution of observed SSTs; however, they differed from each other in their treatment of snow. In the first set, snow depth and its spatial extent were predicted in the GCM integration. In the second set, the climatological annual cycle of snow was specified. For consistency, the annual cycle of the specified snow depth, and its spatial extent, was derived from the first set of GCM simulations. Further, within each set of simulations, three GCM integrations for the 1950–99 period, starting from different atmospheric initial conditions, were conducted.

In the remaining two sets of GCM simulations, instead of specifying observed SSTs, the climatological annual cycle of SSTs was specified. These two sets of GCM simulations also differed from each other in their treatment of snow variability similar to the difference described for the first two sets of GCM simulations. Each set was integrated for 150 yr. This is equivalent to the three 50-yr-long GCM realizations in each of the first two sets of GCM simulations. Hereafter the four sets of GCM simulations are referred to as SST_SNO for the simulations with observed SSTs and predicted snow, SST_CSNO for the simulations with observed SSTs and climatological snow, CSST_SNO for the simulation with climatological SSTs and predicted snow,

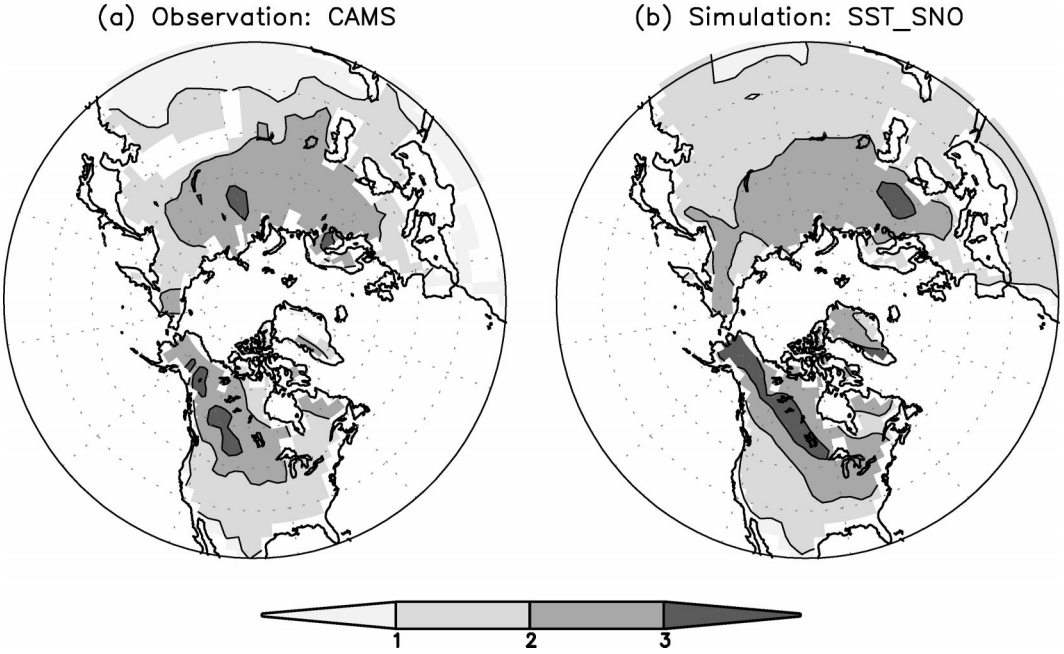

FIG. 1. Std dev of the DJF mean surface air temperatures for (a) observation and (b) GCM simulation. Std dev for the observation is based on the data for the 1950–99 period, whereas std dev for the GCM simulation is derived from three realizations for the 1950–99 period. These GCM simulations are forced with observed SSTs, and snow amount is predicted during the integration (SST_SNO simulation in Table 1). Units are K.

and CSST_CSNO for the simulation with climatological SSTs and climatological snow.

For the GCM simulations, the monthly mean observed SST forcing for the 1950–99 period was obtained from a blended dataset based on two sources. The first was constructed by projecting sparse monthly in situ SSTs over the globe onto empirical orthogonal functions (Smith et al. 1996) for the 1950–80 period. The second was a global SST analysis constructed by combining in situ and satellite observations using an optimum interpolation technique (Reynolds and Smith 1994) for the 1981–99 period.

Interannual variability of temperature and height simulated by the GCM was compared with corresponding observations. For air temperature and height, the NCEP–NCAR (National Center for Atmospheric Research) reanalysis (Kalnay et al. 1996) for the 1950–99 period was used. For surface air temperature, data from the global network of surface observations, Climate Anomaly Monitoring System (CAMS), maintained at NCEP (Ropelewski and Halpert 1986), were utilized. Anomalies for both the GCM simulations and observations were derived from their respective 1950–99 means. Results for the analysis of December–January–February (DJF) seasonal means are discussed in this paper.

3. Results

A comparison of interannual variability of the seasonal mean surface air temperature and 200-hPa heights is shown in Figs. 1 and 2. The purpose of this comparison was to illustrate that the GCM simulations had realistic amplitude of interannual variability. This comparison was based on data from the GCM simulations with predicted snow and forced with observed SSTs (i.e., SST_SNO simulation in Table 1).

Interannual variability of surface air temperature for DJF seasonal means between GCM simulations and observations is compared in Fig. 1. In general, the GCM reproduced the spatial pattern and amplitude of the observed variability. In central to northwestern North America, the largest amplitude of variability was approximately 2.5–3 K in both observations and simulations. Over Eurasia, the largest amplitude of variability was also about of 2.5–3 K. It is also apparent that over Siberia the GCM underestimated the seasonal variability compared to observations.

A comparison of interannual variability of DJF 200-hPa heights between GCM simulations and observations is shown in Fig. 2. Over the Pacific–North American region, GCM-simulated interannual variability matched the observed variability well. However, GCM simulation was less satisfactory over Eurasia where the observed seasonal mean variability was underestimated. This was possibly also the cause for the underestimation of the variability of surface air temperature over Eurasia in Fig. 1. An EOF analysis of seasonal mean heights (see Fig. 7) further confirmed that compared to observations, the amplitude of the North Atlantic Oscillation (NAO) was underestimated by the GCM.

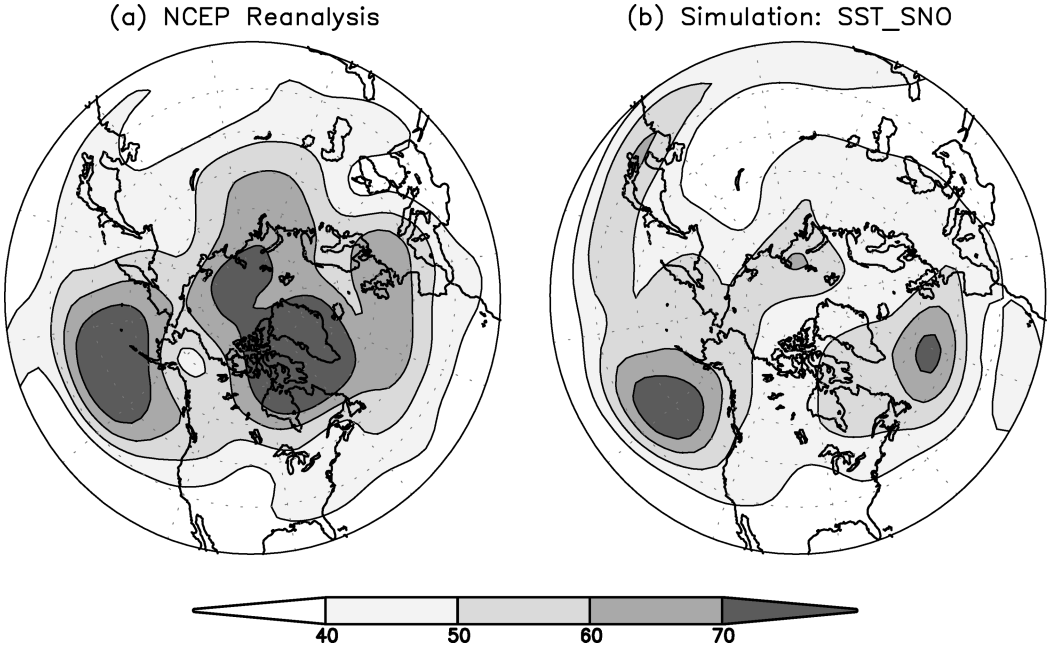

FIG. 2. As in Fig. 1 but for the std dev of the DJF mean 200-hPa heights. Units are m.

Because there are no global observational records long enough to be used for the evaluation of the interannual variability of model simulated snow depth, in Fig. 3 DJF time mean of model-simulated snow depth is compared with a short record of satellite observations. The observed snow depth (Fig. 3a) is derived from the *Nimbus-7* Scanning Multichannel Microwave Radiometer (SMMR) measurements, available from November 1978 to August 1987, based on an algorithm developed by Chang et al. (1987). To be consistent, for both the SMMR and model simulation (SST_SNO), data for the 1979–87 period are used. For the AGCM simulations, to convert water equivalent snow mass to snow depth, the snowpack density is assumed to be 300 kg m^{-3} (Foster et al. 1996). In general, compared to SSMR, the GCM simulation of snow cover extent agrees well over

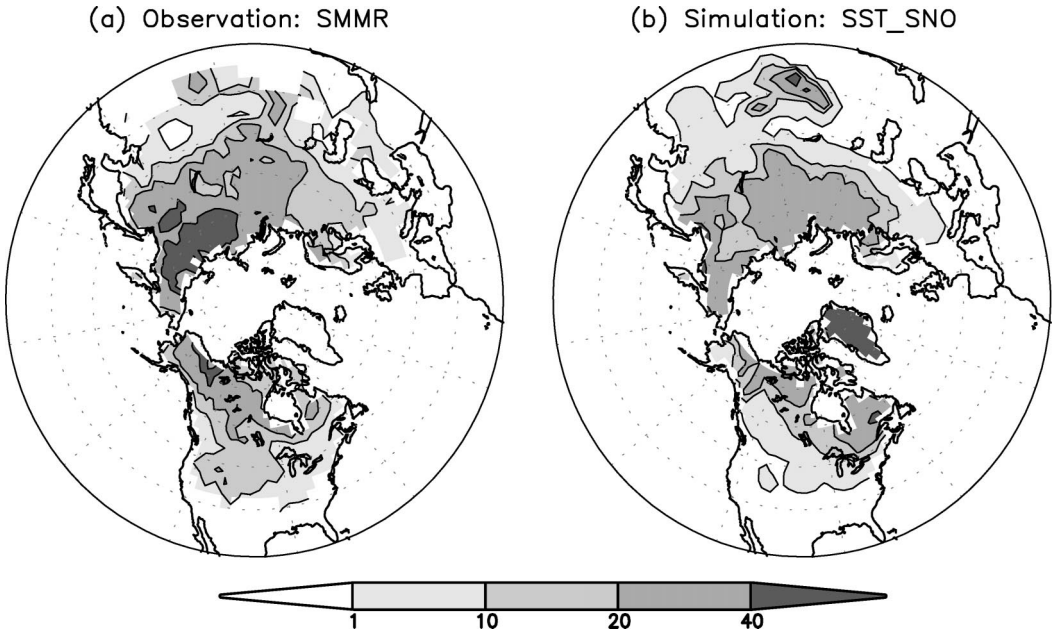

FIG. 3. Snow depth climatology (cm) in DJF derived from (a) the SMMR satellite observations, and (b) model simulation SST_SNO. Both are averages for the 1979–87 period.

Eurasia and over North America. The GCM underestimated snow cover extent and snow mass over central North America, and underestimated snow mass over Alaska and eastern Siberia. Although, because of the shortness of the data record for the observed snow amount, we have not made an explicit comparison of interannual variability between the AGCM and the observed snow amount, comparison of interannual variability of surface temperature in Fig. 1 implicitly includes the influence of interannual snow variability, and gives us confidence in the interannual variability of simulated snow amount (not shown).

The effect of interactive snow on DJF seasonal mean variability is next assessed for surface air temperature and 200-hPa heights. The comparison of two variables at two vertical locations is to illustrate the vertical extent of the effect of snow on atmospheric variability, and to later contrast it with the influence of SST variability. The effect of snow can be assessed from the difference in variability either between SST_SNO and SST_CNSO simulations, or from the difference between CSST_SNO and CSST_CSNO simulations. Results computed both ways are shown in Figs. 4a,b and 5a,b.

For the GCM simulations where interannual variability in snow was allowed, the seasonal variability of surface air temperature increased relative to the GCM simulations where no interannual variability in snow amount occurred (see Figs. 4a and 4b). At some locations this increase was about 30% (e.g., over the northeastern United States). The increases in amplitude and spatial pattern of the surface air temperature variability in Figs. 4a and 4b were similar to each other, and therefore, were independent of the specification of SSTs. The similarity of results between the two sets of GCM simulations also increases our confidence that the results were not an artifact of sampling. It is noteworthy to point out that the largest temperature differences in Figs. 4a and 4b are confined only to certain regions, which have been called temperature-sensitive regions by Karl et al. (1993). Our modeling results are consistent with what Karl et al. (1993) and Groisman et al. (1994) obtained based on observational analyses. A physical explanation of this confinement is given in section 4.

The effect of snow variability on the 200-hPa heights (Figs. 5a and 5b) was much smaller than its effect on surface air temperatures. This is similar to the results of Bladé (1997) and Bhatt et al. (1998). These authors found that the effect of ocean–atmosphere coupling is greater on the variability of near-surface air temperatures than on the variability of upper-tropospheric heights.

To quantify the vertical distribution of the effect of snow variability on the variability of atmospheric seasonal means, longitude–pressure cross sections of the differences in the standard deviations of air temperature between the GCM simulations, with and without snow variability, are shown in Figs. 6a and 6b. The largest differences were concentrated near the surface, and consistent with the spatial patterns in Fig. 4, were stronger over the longitudes corresponding to North America. The vertical structure of the difference in atmospheric temperature variability suggests that the effect of snow variability was indeed confined near the surface, and did not alter the atmospheric variability of the upper-atmospheric circulation.

We next consider whether the interactive snow variability may also have some effect on the spatial structures of preferred modes of atmospheric variability. For this analysis, modes of interannual variability of 200-hPa seasonal mean heights obtained from the rotated empirical orthogonal function (EOF) technique were compared among different GCM simulations. The analysis used 150 yr of DJF seasonal mean heights over the latitudes north of 25°N.

A comparison of the leading modes of atmospheric variability in the SST_SNO simulations was made with the modes of atmospheric variability in the SST_CSNO simulations. These results are shown in Fig. 7 where the spatial patterns of the leading modes of atmospheric variability for the SST_SNO simulations (left panels) are paired with the modes of atmospheric variability for the SST_CSNO simulations (right panels).

The leading mode of 200-hPa DJF seasonal mean heights in the SST_SNO simulations was the Pacific–North American (PNA) pattern. This was also the leading mode of variability in the SST_CSNO simulations, and therefore, the effect of snow variability did not change the spatial pattern of the leading mode of atmospheric height variability. The spatial pattern of the second mode in the SST_SNO simulations was found to be the fourth mode in the SST_CSNO simulations. Similarly mode 3(4) in the SST_SNO simulations was closely related to mode 2(5) in the SST_CSNO simulations. This implies that without changing the spatial structure of the modes of atmospheric variability appreciably, the effect of snow variability was primarily on the reordering of these modes. This was further evident from the spatial correlations between the left and right pairs of modes in Fig. 7, which were always larger than 0.9.

This reordering of the leading modes of variability was similar to the result of an earlier study of Bladé (1997) in which the effect of ocean–atmosphere coupling on the modes of atmospheric low-frequency variability was investigated. From Fig. 7 it is also apparent that, whereas for observations the NAO is the leading mode and explains approximately 21% of the DJF variability (not shown), in the GCM simulations this fraction was only about 7% (the bottom panels in Fig. 7), indicating that variability of this mode was severely underestimated.

For analyses in Figs. 4–6, we next contrast the effect of interannual variations in SSTs with the effect of interannual variations in snow on the variability of extratropical atmospheric flow. As for the influence of snow on atmospheric variability, the influence of SSTs can

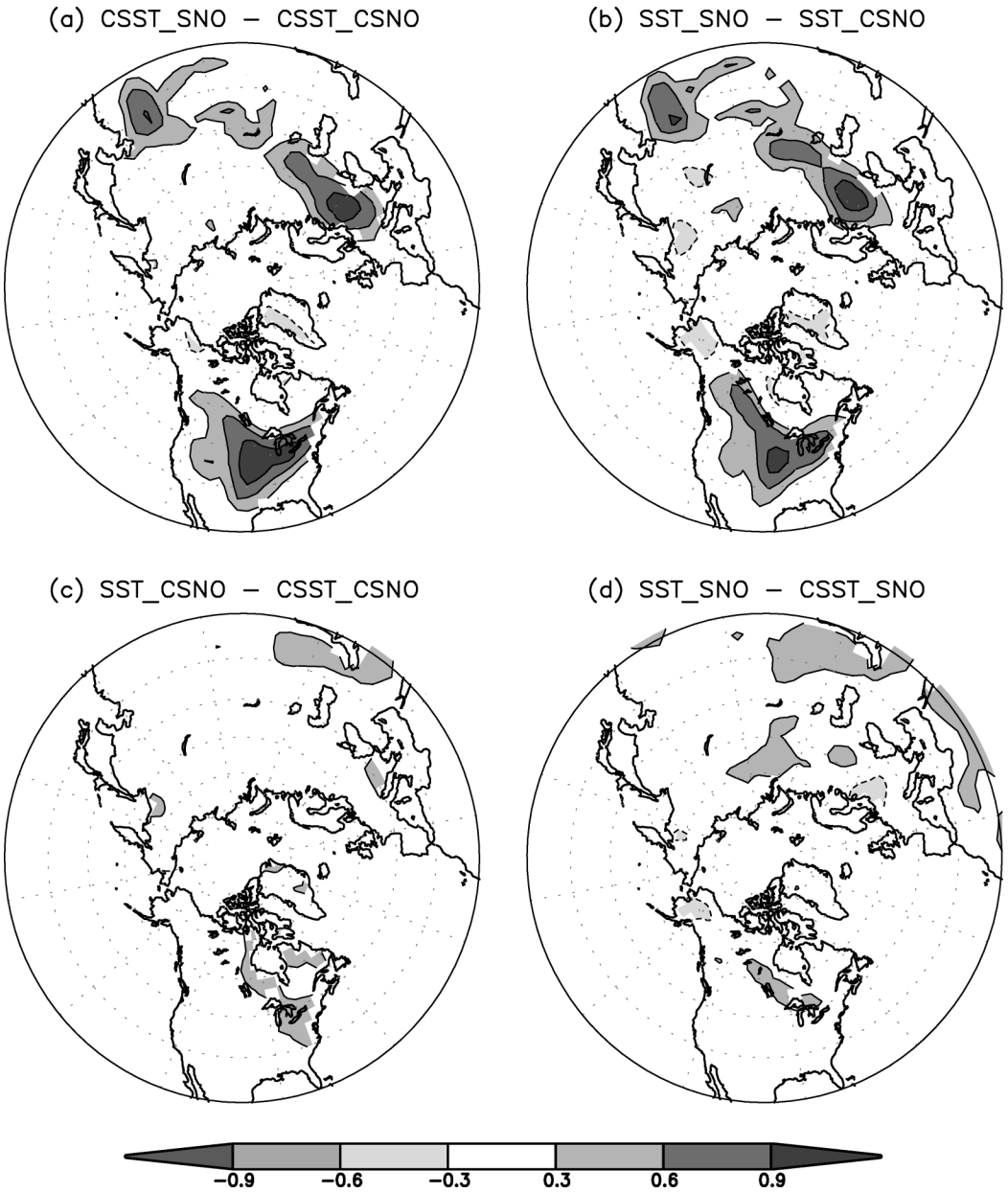

FIG. 4. Difference in the std dev of the DJF mean surface air temperatures between the various sets of GCM simulations in Table 1. (a), (b) The influence of snow variability; (c), (d) the influence of SST variability. Contour interval is 0.3 K. Dashed contours are for negative values. Zero contour is omitted. Data over the oceans are masked for a better comparison.

also be computed in two ways: 1) by comparing SST_CSNO and CSST_CSNO simulations, or 2) by comparing SST_SNO and CSST_SNO simulations. The results computed both ways are shown. We should point out that although the GCM simulations were forced with global distributions of the observed SSTs, we expect that it is the interannual variations of SSTs in the tropical Pacific related to ENSO that have the largest influence on the extratropical atmospheric variability (Bladé 1997; Saravanan 1998).

The influence of SST variability on the variability of surface air temperature (Figs. 4c and 4d) was small. Furthermore, it was much smaller than the corresponding influence of snow variability (Figs. 4a and 4b). For the variability of 200-hPa heights, on the other hand, the influence of SST variability was much larger than that of snow variability (see Fig. 5). In general, the amplitude of 200-hPa seasonal mean height variability was larger in the GCM simulations with the interannual variability in SSTs than that without the interannual var-

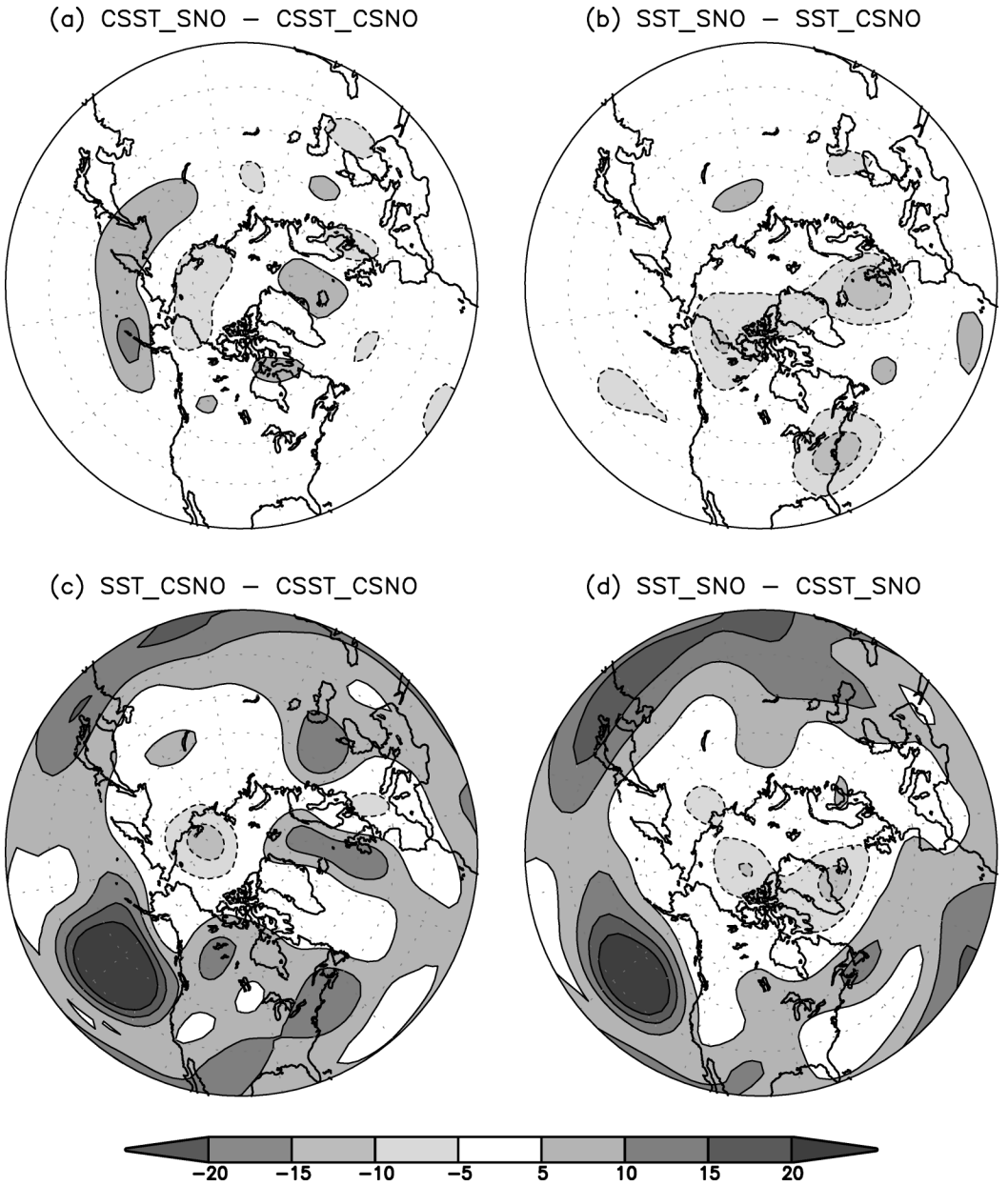

FIG. 5. As in Fig. 4 but for the std dev of the DJF mean 200-hPa heights. Contour interval is 5 m.

iability in SSTs. The largest increase in variability in the extratropical latitudes was located south of Alaska, which was also the center of the largest atmospheric response to the tropical Pacific SSTs (e.g., see Figs. 8a and 8c for the atmospheric response to the tropical Pacific SSTs).

The vertical characteristics of the influence of SSTs on the extratropical seasonal mean variability, therefore, was the reverse of the influence of the interannual variability of snow. Compared to the influence of snow variability, the interannual variability of SSTs had less influence closer to the surface, and larger influence in the upper troposphere. This is also apparent in Figs. 6c and 6d where the longitude–pressure cross sections of the difference of seasonal mean temperature variability associated with SST variability are shown. In contrast to the vertical structure of the atmospheric influence of snow (Figs. 6a and 6b), which was confined to the lower troposphere, the influence of SST tends to spread throughout the deep troposphere, and at times are larger in the upper troposphere.

To summarize, the comparison of the influence of interannual variability of SSTs and snow on extratropical climate demonstrated contrasting behavior. This is possibly due to differing mechanisms through which SSTs and snow influence atmospheric variability in the

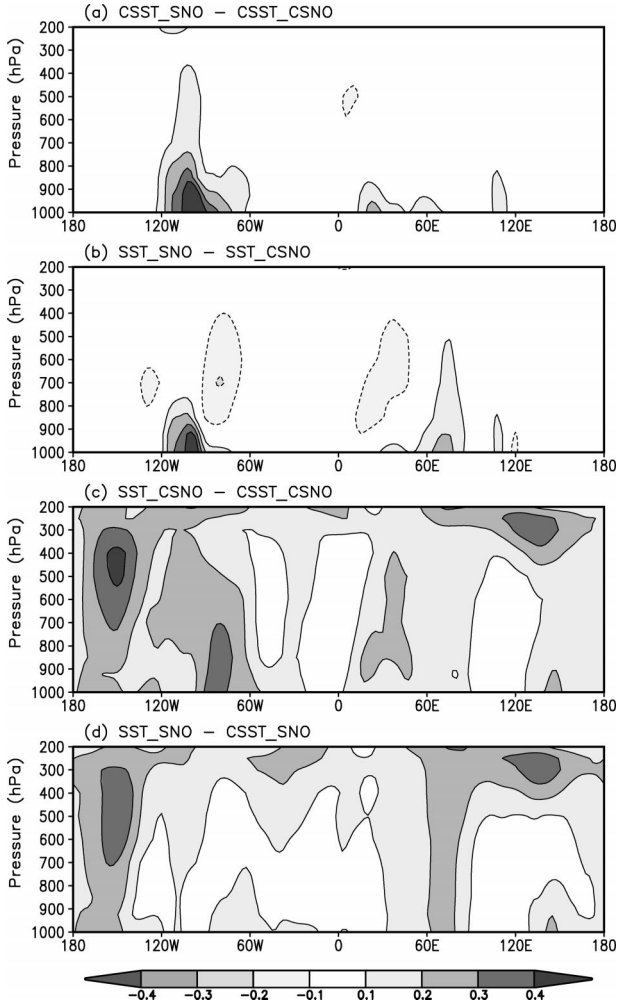

FIG. 6. Lon–pressure cross sections of the difference in the std dev of the DJF mean air temperatures between various sets of GCM simulations in Table 1. Difference in the std dev was meridionally averaged from 30° to 60°N. (a), (b) The impact of snow variability; (c), (d) show the impact of SST variability. Contour interval is 0.1 K, and the zero contour is omitted. Dashed contours are for negative values.

extratropics. Atmospheric response to tropical Pacific SSTs occurs through changes in convective patterns in the tropical latitudes, which alter the upper-level divergent circulation and generate anomalous Rossby wave sources. The influence of this travels to the extratropical latitudes in the upper troposphere (Sardeshmukh and Hoskins 1988; Trenberth et al. 1998). This remote response to tropical SSTs in the extratropical latitudes is further manifested as an equivalent barotropic structure. The physical processes involved in the influence of snow variability, on the other hand, take place near the surface and their influence subsequently has to propagate into the upper troposphere. Thus, the top-down mechanism of the influence of the tropical SSTs and the bottom-up mechanism of the influence of snow on extratropical atmospheric variability may explain the differing vertical structure of the atmospheric response to SSTs and snow.

Another question that the GCM simulations can help answer is how the snow variability modulates the remote response to SSTs. Comparisons of surface air temperature in Figs. 4c with Fig. 4d, and height variability in Figs. 5c with Fig. 5d, indicate that the overall influence of SST, either with or without snow variability, was very similar. Insensitivity of the influence of SSTs on upper-level heights to the specification of snow is easy to understand because the influence of snow variability is small in the upper troposphere. To understand the apparent insensitivity of the influence of SSTs on surface air temperature to the specification of snow, we should point out that (i) large SST anomalies in the tropical Pacific do not occur every year in the data record, and (ii) any snow influence for those selective years when tropical Pacific SST anomalies related to ENSO do occur, can be obscured by the large internal variability during the remaining years. The combined influence of these two is such that the analysis of variance of surface temperatures over all the years is not able to identify the feedback from the snow variability during the years of large anomalous SSTs alone.

A better way to demonstrate the modulation of the influences of tropical SSTs on extratropical climate by snow is to focus on those years alone when large tropical Pacific SST anomalies occur, and compare the atmospheric response of SSTs in GCM simulations with and without the interannual variability of snow. Following this approach Yang et al. (2001), based on composite analysis, demonstrated that the variability in snow amount indeed amplified the extratropical surface air temperature response to tropical SST anomalies during ENSO years. A similar analysis, based on regressions with the Niño-3.4 (5°S–5°N, 170°–120°W) SST index, is used to demonstrate the effect of snow variability on the remote response in the atmosphere to tropical SSTs. Regression maps for surface air temperature and 200-hPa heights for the SST_SNO and SST_CSNO simulations are shown in Fig. 8.

For 200-hPa heights, as expected, the two regression maps (Figs. 8a and 8c) are very similar. On the other hand, consistent with the result of Yang et al. (2001), the amplitude of surface air temperature regression in the SST_SNO simulation (Fig. 8d) was stronger than that in the SST_CSNO simulations (Fig. 8b). As a consequence, the remote response in the surface air temperature to tropical Pacific SSTs in the absence of snow variability (i.e., surface temperature regression for the SST_CSNO simulations) was amplified when the interaction between the atmosphere and underlying snow was allowed.

4. Physical mechanism for the influence of snow on atmospheric variability

In the previous section, from the analysis of GCM simulations with differing specifications of snow, we

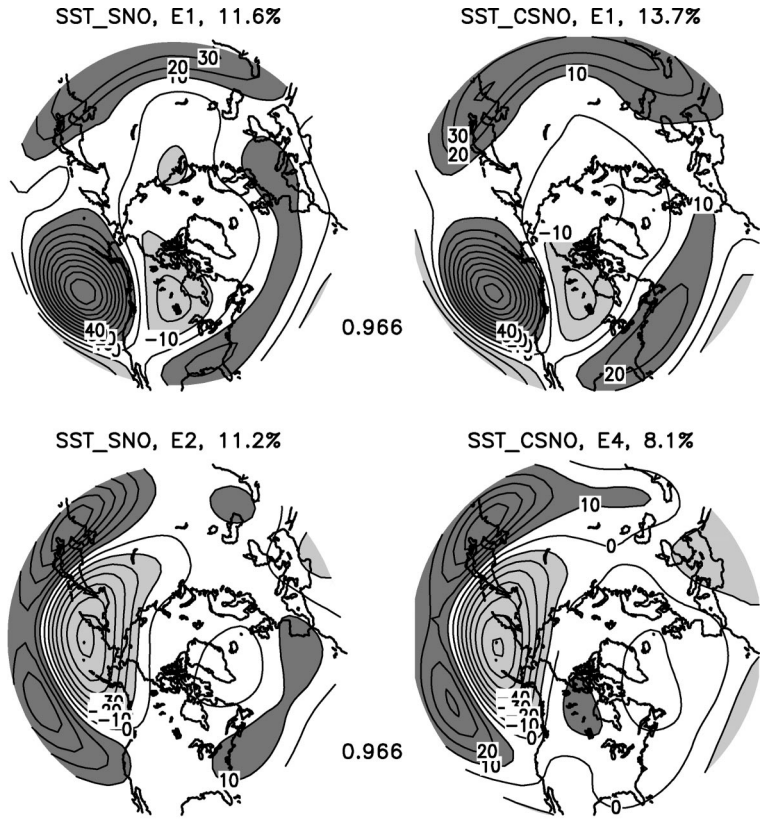

FIG. 7. (left) Spatial patterns of the first four rotated EOFs for 200-hPa seasonal mean DJF heights for the GCM simulations forced with the observed SSTs and predicted snow (SST_SNO simulations in Table 1). (right) These modes were paired with the similar modes for the SST_CSNO simulations where annual cycle of snow was specified. The numerical value at the top of each panel is the percent variance

demonstrated that inclusion of snow variability led to an increase in seasonal mean atmospheric variability, particularly in the lower troposphere. In this section, a physical explanation for this influence is discussed. The effects of snow cover on the surface temperature and energy balance have been discussed extensively in literature (e.g., Cohen and Rind 1991; Groisman et al. 1994; Cess et al. 1991). Cohen and Rind (1991) describes different mechanisms by which snow can alter surface energy balance, and can influence lower-tropospheric temperatures. Included among them is the influence of snow on the surface albedo. Overall, snow can contribute toward increasing the surface temperature variability because of a potential positive snow–albedo feedback. In our GCM, surface albedo over snow-covered surface is parameterized and depends on snow depth amount (Briegleb 1992; Yang et al. 2001). Surface albedo increases with an increase in snow amount (see the appendix). Changes in surface albedo with snow amount alter the surface absorption of downward solar radiation, and therefore, influence surface energy balance, which can lead to an enhancement of the surface temperature anomalies.

To elaborate, consider an initial warm temperature anomaly near the surface. This anomaly could be either due to the atmospheric internal variability, or to the influence of SSTs, for example, tropical Pacific SSTs. Warm temperature anomalies will lead to snowmelt and reduce snow depth amount. This will result in a reduction of the surface albedo and an increase in the surface absorption of solar radiation. Increased absorption of solar radiation, in turn, warms the surface temperatures. This warming is quickly communicated to the near-surface air temperatures, leading to further enhancement of the initial air temperature anomaly. Warmer surface and air temperatures, in turn, lead to further snowmelts. The reverse happens for the cold temperature anomalies.

This positive feedback between the atmosphere and snow variability is responsible for the increase in the variability of seasonal mean tropospheric temperatures found in the analysis in the previous section. Although a positive feedback, the influence of snow on atmospheric variability remains bounded because the rate of increase in surface albedo decreases as snow depth increases. Thus, for large mean snow amounts, changes in snow depth around it do not alter the magnitude of surface albedo further, and therefore, there is an intrinsic mechanism for the positive feedback to self-regulate.

Functional dependence of surface albedo on snow depth, and the meridional distribution of downward solar radiation in boreal winter, also puts constraints on the geographical locations where the influence of in-

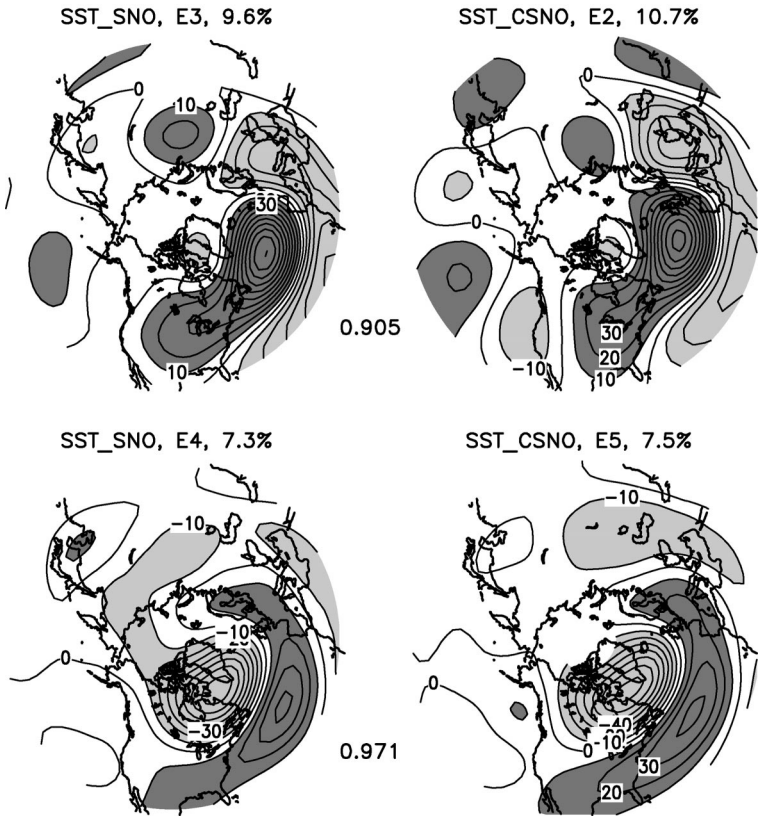

Fig. 7. (*Continued*) explained by the mode. Pattern correlation between the left and right pair is shown in the middle. Spatial pattern is shown as the regression of 200-hPa heights with the time series of the principle components of the rotated EOFs. The EOF analysis was performed for the spatial domain shown in the figure.

terannual variability in snow on the atmospheric variability can occur. For example, for extreme northern latitudes, the downward surface insolation at the surface is small, and therefore, any changes in snow amount and surface albedo will not influence atmospheric variability. Similarly for the locations where climatological snow amount is large, interannual changes in snow amount around this mean will not change surface albedo, and therefore, will not influence atmospheric variability either.

To illustrate the geographical preference for the influence of snow variability on the atmospheric flow, we start from the spatial pattern of interannual variability in snow amount. This, for the SST_SNO simulations, is shown in Fig. 9a. In general, the variability reached maximum in the northern latitudes. The maximum of the interannual variability in surface albedo (Fig. 9b) was not collocated with the maximum of the interannual variability in the snow amount, but was shifted southward. This is also apparent from the comparison of the zonal means of the interannual variability in snow depth amount and surface albedo shown in Fig. 10. The reason for the southward shift of the variability in surface albedo is because the interannual snow variability in the northernmost latitudes is superimposed upon a large climatological snow amount, and therefore, cannot generate appreciable surface albedo variability.

The interannual variability of the reflected solar radiation at the surface, which is the product of surface insolation and surface albedo, was shifted farther southward (see Figs. 9c and 10). This is because of the northward decrease of solar insolation in DJF. The spatial distribution of the interannual variability of downward surface solar radiation (Fig. 9d) also confirms that the variation in the reflected surface solar radiation was not caused by changes in downward surface solar radiation. This is also apparent from the similarity in the spatial patterns of interannual variability in surface albedo and the reflected solar radiation. This implies that the main contributor to the variability in the reflected solar radiation is the variability in surface albedo. Interannual variability in reflected solar radiation in the SST_SNO simulations then leads to changes in the interannual variability of surface temperature in Fig. 4. This demonstrates how the dependence of surface albedo on snow depth amount, together with the latitudinal variation of solar insolation, can lead to preferred locations where interannual variations in snow amount can influence atmospheric variability.

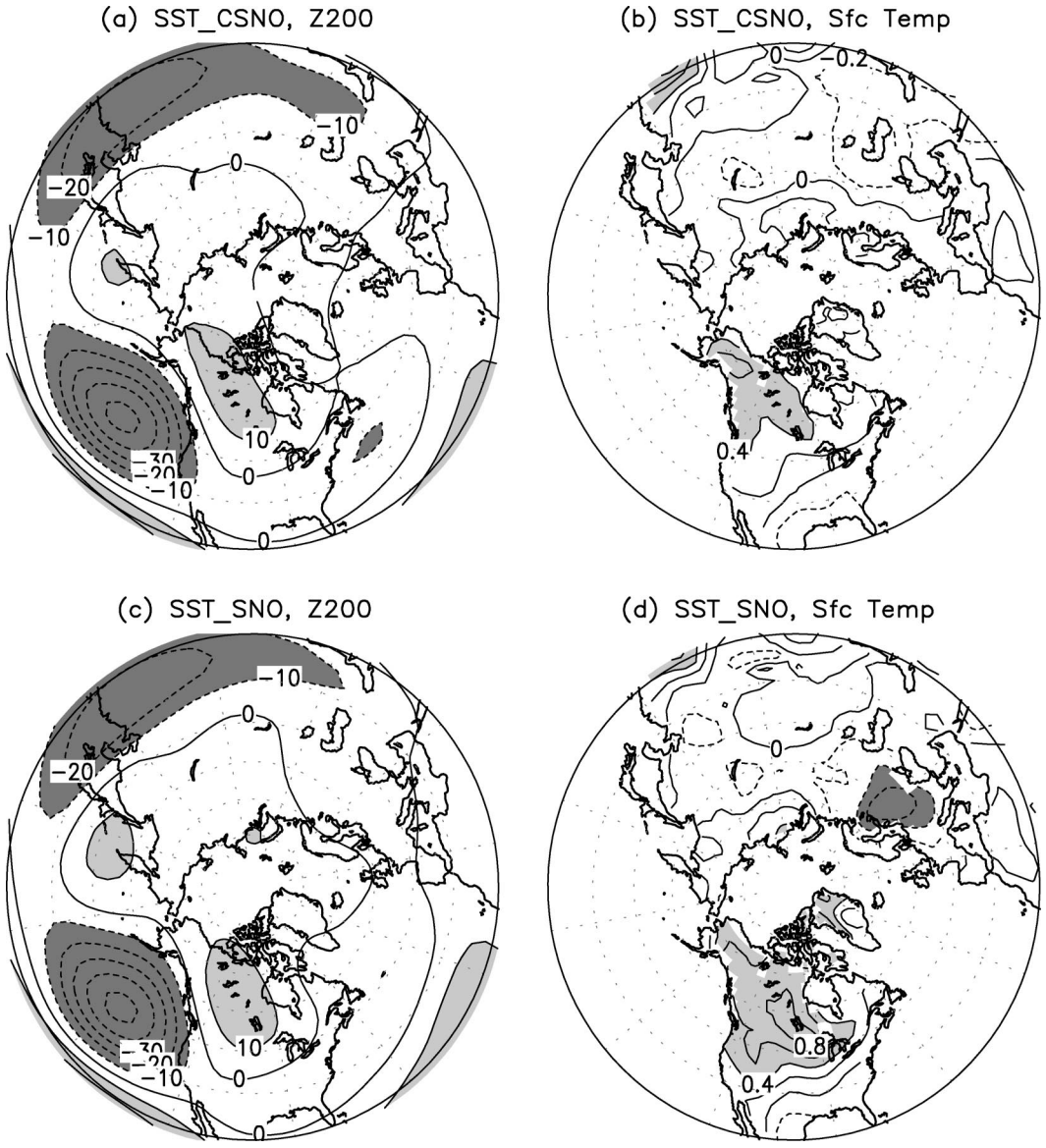

FIG. 8. Linear regressions of (a), (c) 200-hPa seasonal mean DJF heights and (b), (d) surface air temperatures with the Niño-3.4 SST index for the 1950–99 period. For these regressions, the ensemble mean of the three GCM simulations were used. (a), (b) The GCM simulations with specified annual cycle of snow; (c), (d) the GCM simulations with interactive snow (see Table 1 for the definitions of the GCM simulations). Spatial maps are shown for unit std dev of the Niño-3.4 SST index. Comparison of (a), (b) and (c), (d) indicates the influence of snow feedback on the extratropical atmospheric response to tropical Pacific SSTs. Contour interval is 10 m for height, and 0.2 K for temperature.

5. Summary

In this paper the influence of snow variability on the atmosphere in the Northern Hemisphere extratropical latitudes in boreal winter was analyzed. The analysis was of relevance toward understanding the interannual variability of seasonal mean atmospheric states. It was based on a series of GCM simulations forced with differing specifications for the interannual variability of snow. The influence of snow on the atmospheric variability was also compared with the similar influence of SST variability.

Results indicated that near the surface, snow variability leads to an increase in the variability of seasonal mean atmospheric temperature. However, this effect was confined to the lower troposphere. Further, the influence of snow variability did not change the spatial patterns of the dominant modes of atmospheric low-frequency variability. The physical mechanism for the influence of snow variability on atmospheric temperature was argued to be the dependence of surface albedo on snow depth amount, and corresponding changes in the surface energy balance.

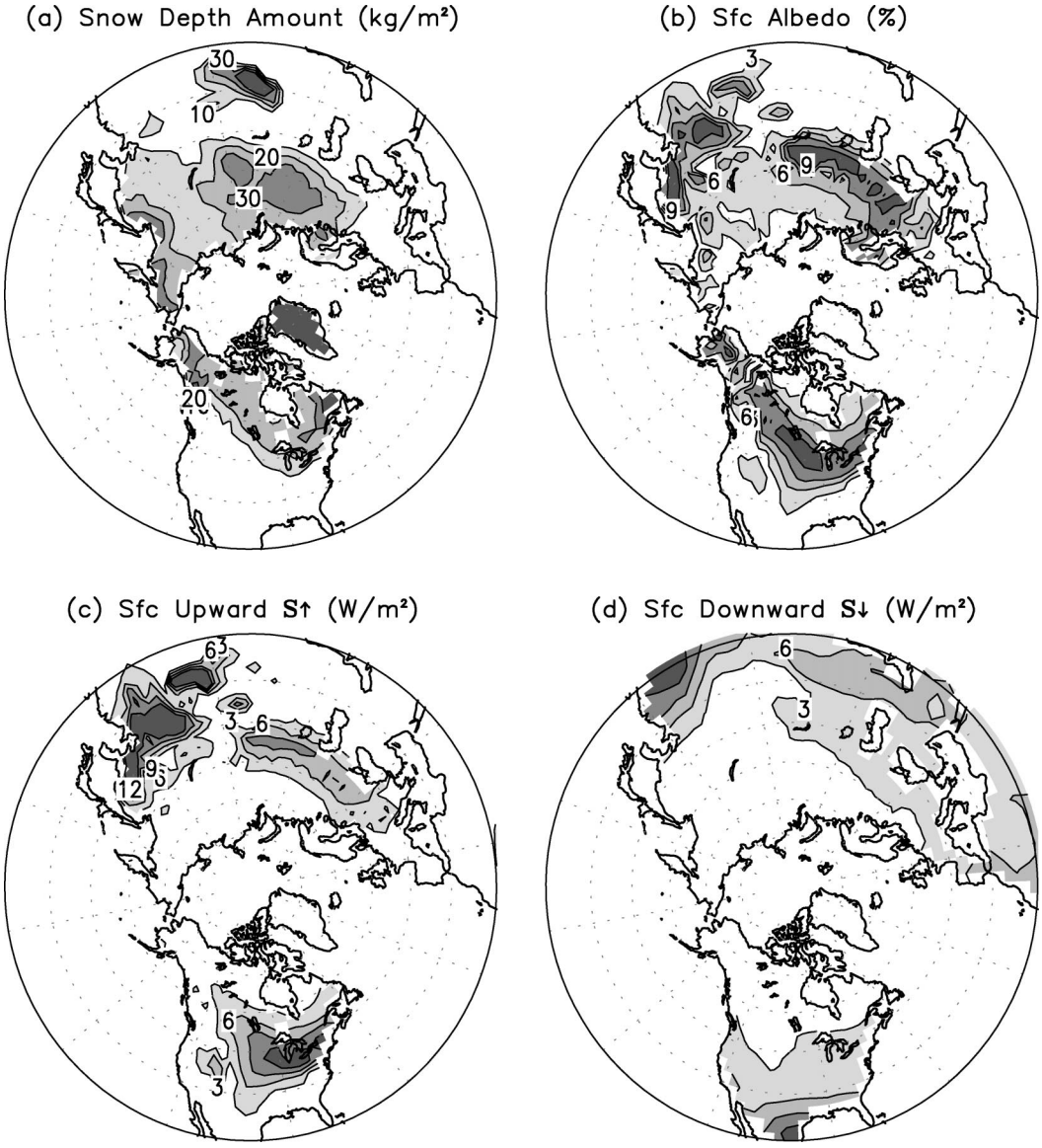

FIG. 9. Std dev of DJF means for (a) water equivalent of snow depth amount (kg m^{-2}), (b) surface albedo (%), (c) reflected upward solar radiation at the surface (W m^{-2}), and (d) downward solar radiation at the surface (W m^{-2}). Results are obtained from the GCM simulations forced with the observed SSTs and predicted snow (SST_SNO simulations in Table 1), and demonstrate differences in spatial structure in the interannual variability for different variables. Contour interval is 10 in (a), and 3 in (b)–(d).

In terms of a simple mechanistic model, the influence of snow variability on atmospheric flow can be described in the following manner: In the atmosphere, even in the absence of any interannual variability in snow amount, internal modes of low-frequency atmospheric variability exist (e.g., in the CSST_CSNO simulation). These modes of atmospheric variability are also associated with temperature anomalies in the lower troposphere. If the snow amount is allowed to vary, as for the CSST_SNO simulations, temperature anomalies are further amplified because of the dependence of surface albedo on snow amount. A similar mechanism also enhances the effect of tropical SST anomalies on the extratropical surface temperature variability (Yang et al. 2001). For this case, however, initial lower-tropospheric temperature anomalies are due to the remote SST forcing instead of atmospheric internal variability.

Comparing the influence of snow variability on the atmosphere with that of SST variability, it was found that their vertical structure in the extratropical latitudes differed. The influence of snow was a more surface-to-upper-troposphere response, while the influence of SSTs was upper-troposphere-to-surface in its character. The surface-to-upper-troposphere effect of snow variability

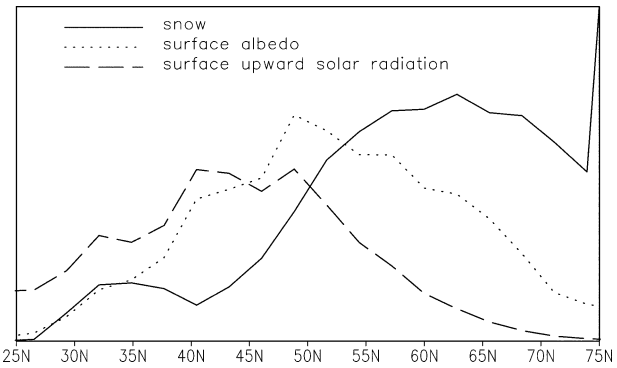

FIG. 10. Lat distribution of the zonal mean of the std dev for water equivalent of snow depth (solid line), surface albedo (dashed line), and surface upward solar radiation (dashed line). Different variables are scaled for a better comparison of their lat distribution.

is also similar to the effect of soil moisture anomalies on atmospheric circulation in boreal summer (Wang and Kumar 1998), and is also similar to the effect of extratropical ocean variability on atmospheric seasonal means (Bladé 1997; Bhatt et al. 1998).

Although the vertical structure of the influence of snow on atmospheric variability was similar to that of extratropical oceans, the physical mechanism for the influence of snow variability was not just the thermal damping mechanism, which, for the case of coupled ocean–atmosphere interactions, is responsible for the increase of variance on seasonal timescales. The mechanism of influence of snow variability, in addition, was related to changes in the properties of the land surface, that is, surface albedo. There is no counterpart for this in the ocean–atmosphere interactions; that is, ocean–atmosphere interactions do not lead to changes in the physical properties of the ocean surface.

Our analysis was based on the simulations of a single GCM. Because the parameterization of surface albedo on snow amount changes from one GCM to another (e.g., see Watanabe and Nitta 1998; Betts 2000; Yang et al. 2001), it is possible that results, to a certain extent, may be model dependent. However, from the physical considerations of how the interaction between snow depth and surface albedo influences the atmospheric variability, we expect that qualitatively our results will also hold for other GCMs.

Because the influence of snow variability also modulates the remote response of the extratropical atmosphere to tropical Pacific SSTs, and because different GCMs have different parameterizations of surface albedo on snow depth, the local feedback through which snow variability modulates the ENSO response of the atmosphere may vary among different GCMs. Therefore, GCMs that might have similar upper-tropospheric response to tropical SSTs may still differ in their surface responses.

Finally, in the present study we did not analyze the predictability aspects of snow variability on seasonal atmospheric means. Understanding and documenting the influence of snow variability on atmospheric variability is a necessary first step toward analyzing the predictability aspects of snow. For if such influences are found, initial anomalies in snow may have an influence on the subsequent monthly and seasonal atmospheric means, and therefore, could be of some predictive value (Cohen and Entekhabi 1999).

Acknowledgments. This work was supported by the National Ocean and Atmospheric Administration's Climate Dynamics and Experimental Prediction Program. We thank Dr. Wanqiu Wang for useful discussions. The final version of this manuscript greatly benefited from the comments by two anonymous reviewers.

APPENDIX

Parameterization of Surface Albedo in the NCEP GCM

In the NCEP GCM used in this study, grid-averaged surface albedo over snow-covered land for each broad band of solar radiation is given by (Briegleb 1992)

$$\alpha = \alpha_{\text{land}}(1 - f_{\text{snow}}) + \alpha_{\text{snow}} f_{\text{snow}}, \qquad \text{(A1)}$$

where α_{land} is the albedo for snow free surface, which is estimated from observations and depends on solar zenith angle. Further, the fractional snow cover f_{snow} is defined as

$$f_{\text{snow}} = \text{SCV}/(\text{SCV} + R), \qquad \text{(A2)}$$

where SCV is snow depth in meters, and R the aerodynamic roughness of the underlying surface that varies from 0.025 to 1.0 m. Finally, surface albedo for the snow-covered surface is defined separately for the direct and diffuse incident solar radiation. For direct incident solar radiation

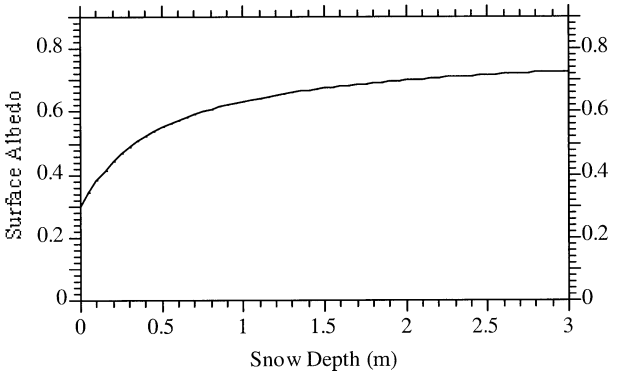

FIG. A1. Land surface albedo as a function of snow depth. For specific values of parameters used in computation see the text.

$$\alpha_{\text{snow}} = \begin{cases} \alpha^0_{\text{snow}} + (1 - \alpha^0_{\text{snow}})\left[0.5\left(\dfrac{3}{1 + 4\cos\zeta} - 1\right)\right], \\ \qquad 0 \le \cos\zeta \le 0.5 \\ \alpha^0_{\text{snow}}, \qquad \cos\zeta \ge 0.5, \end{cases} \tag{A3}$$

where ζ is the solar zenith angle. For diffuse incident solar radiation $\alpha_{\text{snow}} = \alpha^0_{\text{snow}}$. Here α^0_{snow} is prescribed to observed spectral snow albedo, and is much larger than albedo over the land α_{land}.

To illustrate how surface albedo varies with snow depth, we consider a special case. Assume $\alpha_{\text{land}} = 0.3$, $\alpha^0_{\text{snow}} = 0.8$, $R = 0.5$, and $\zeta = 0°$, then $\alpha_{\text{snow}} = \alpha^0_{\text{snow}}$,

$$f_{\text{snow}} = \text{SCV}/(\text{SCV} + 0.5), \tag{A4}$$

$$\alpha = 0.3(1 - f_{\text{snow}}) + 0.8 f_{\text{snow}}. \tag{A5}$$

For this choice of parameters, surface albedo, as a function of snow depth, is shown in Fig. A1. Surface albedo increases rapidly for a small amount of snow depth. The rate of increase, however, decreases for larger snow amounts. For a large snow amount, surface albedo has very little increase with increasing snow amounts.

REFERENCES

Barnett, T. P., L. Dümenil, U. Schlese, and R. Rockner, 1998: The effect of Eurasian snow cover on global climate. *Science*, **239,** 504–507.

Barsugli, J. J., and D. S. Battisti, 1998: The basic effects of atmosphere–ocean thermal coupling on midlatitude variability. *J. Atmos. Sci.*, **55,** 477–493.

Betts, R. A., 2000: Offset of the potential carbon sink from boreal forestation by decreases in surface albedo. *Nature,* **408,** 187–190.

Bhatt, U. S., M. A. Alexander, D. S. Battisti, D. D. Houghton, and L. M. Keller, 1998: Atmosphere–ocean interaction in the North Atlantic: Near-surface climate variability. *J. Climate,* **11,** 1615–1632.

Bladé, I., 1997: The influence of midlatitude ocean–atmosphere coupling on the low-frequency variability of a GCM. Part I: No tropical SST forcing. *J. Climate,* **10,** 2087–2106.

Briegleb, B., 1992: Delta-Eddington approximation for solar radiation in the NCAR community climate model. *J. Geophys. Res.,* **97,** 7603–7612.

Cess, R. D., and Coauthors, 1991: Interpretation of snow–climate feedback as produced by 17 general circulation models. *Science,* **253,** 888–892.

Chang, A. T. C., J. L. Foster, and D. K. Hall, 1987: *Nimbus-7* SMMR derived global snow cover parameters. *Ann. Glaciol.,* **9,** 39–44.

Clark, M. P., M. C. Serreze, and D. A. Robinson, 1999: Atmospheric controls on Eurasian snow extent. *Int. J. Climatol.,* **19,** 27–60.

Cohen, J., and D. Rind, 1991: The effect of snow on the climate. *J. Climate,* **4,** 689–706.

——, and D. Entekhabi, 1999: Eurasian snow cover variability and Northern Hemisphere climate predictability. *Geophys. Res. Lett.,* **26,** 345–348.

——, and ——, 2001: The influence of snow cover on Northern Hemisphere climate variability. *Atmos.–Ocean,* **39,** 35–53.

Foster, J., and Coauthors, 1996: Snow cover and snow mass intercomparisons of general circulation models and remotely sensed datasets. *J. Climate,* **9,** 409–426.

Gallimore, R. G., 1995: Simulated ocean–atmosphere interaction in the North Pacific from a GCM coupled to a constant-depth mixed layer. *J. Climate,* **8,** 1721–1737.

Groisman, P. Ya., T. R. Karl, and R. W. Knight, 1994: Changes of snow cover, temperature, and radiative heat balance over the Northern Hemisphere. *J. Climate,* **7,** 1633–1656.

Kalnay, E., and Coauthors, 1996: The NCEP/NCAR 40-Year Reanalysis Project. *Bull. Amer. Meteor. Soc.,* **77,** 437–471.

Kanamitsu, M., and Coauthors, 2002: NCEP dynamical seasonal forecast system 2002. *Bull. Amer. Meteor. Soc.,* **83,** 1019–1037.

Karl, T. R., P. Ya. Groisman, R. W. Knight, and R. R. Heim Jr., 1993: Recent variations of snow cover and snowfall in North America and their relations to precipitation and temperature variations. *J. Climate,* **6,** 1327–1344.

Kushnir, Y., W. A. Robinson, I. Bladé, N. M. J. Hall, S. Peng, and R. Sutton, 2002: Atmospheric GCM response to extratropical SST anomalies: Synthesis and evaluation. *J. Climate,* **15,** 2233–2256.

Lau, N.-C., and M. J. Nath, 1996: The role of the ''atmospheric bridge'' in linking tropical Pacific ENSO events to extratropical SST anomalies. *J. Climate,* **9,** 2036–2057.

Reynolds, R. W., and T. M. Smith, 1994: Improved global sea surface temperature analyses using optimum interpolation. *J. Climate,* **7,** 929–948.

Ropelewski, C. F., and M. S. Halpert, 1986: North America precipitation and temperature patterns associated with the El Niño/Southern Oscillation (ENSO). *Mon. Wea. Rev.,* **114,** 2352–2362.

Saravanan, R., 1998: Atmospheric low-frequency variability and its relationship to midlatitude SST variability: Studies using the NCAR Climate System Model. *J. Climate,* **11,** 1388–1406.

Sardeshmukh, P. D., and B. J. Hoskins, 1988: The generation of global rotational flow by steady idealized tropical divergence. *J. Atmos. Sci.,* **45,** 1228–1251.

Smith, T. M., R. W. Reynolds, R. E. Livezey, and D. C. Stokes, 1996: Reconstruction of historical sea surface temperature using empirical orthogonal functions. *J. Climate,* **9,** 1403–1420.

Trenberth, K. E., G. Branstator, G. W. Karoly, A. Kumar, N.-C. Lau, and C. Ropelewski, 1998: Progress during TOGA in understanding and modeling global teleconnections with tropical sea surface temperatures. *J. Geophys. Res.,* **103,** 14 291–14 324.

Walland, D. J., and I. Simmons, 1997: Association between modes of variability of January Northern Hemisphere snow cover and circulation. *Theor. Appl. Climatol.,* **58,** 187–210.

Walsh, J. E., and B. Ross, 1988: Sensitivity of 30-day dynamical forecasts to continental snow cover. *J. Climate,* **1,** 739–754.

Wang, W., and A. Kumar, 1998: A GCM assessment of atmospheric seasonal predictability associated with soil moisture anomalies over North America. *J. Geophys. Res.,* **103,** 28 637–28 646.

Watanabe, M., and T. Nitta, 1998: Relative impacts of snow and sea surface temperature anomalies on an extreme phase in the winter atmospheric circulation. *J. Climate,* **11,** 2837–2857.

Yang, F., A. Kumar, W. Wang, H.-M. H. Juang, and M. Kanamitsu, 2001: Snow–albedo feedback and seasonal climate variability over North America. *J. Climate,* **14,** 4245–4248.